Extensive Nuclear Reprogramming Underlies Lineage Conversion into Functional Trophoblast Stem-like Cells

Benchetrit, Hana; Herman, Shay; van Wietmarschen, Niek; Wu, Tao; Makedonski, Kirill; Maoz, Noam; Tov, Nataly Yom; Stave, Danielle; Lasry, Rachel; Zayat, Valery

Published in:
Cell stem cell

DOI:
10.1016/j.stem.2015.08.006

Cell Stem Cell
Article

Extensive Nuclear Reprogramming Underlies Lineage Conversion into Functional Trophoblast Stem-like Cells

Hana Benchetrit,[1] Shay Herman,[1] Niek van Wietmarschen,[2] Tao Wu,[3] Kirill Makedonski,[1] Noam Maoz,[1] Nataly Yom Tov,[1] Danielle Stave,[1] Rachel Lasry,[1] Valery Zayat,[1] Andrew Xiao,[3] Peter M. Lansdorp,[2,4] Shulamit Sebban,[1] and Yosef Buganim[1,*]

[1]Department of Developmental Biology and Cancer Research, The Institute for Medical Research Israel-Canada, The Hebrew University-Hadassah Medical School, Jerusalem 91120, Israel
[2]European Research Institute for the Biology of Ageing, University Medical Center Groningen, University of Groningen, Antonius Deusinglaan 1, AV Groningen 9713, the Netherlands
[3]Yale Stem Cell Center and Department of Genetics, Yale University, New Haven, CT 06520, USA
[4]Skolkovo Institute of Science and Technology (Skoltech), Novaya str. 100, Skolkovo Moscow Region 143025, Russia
*Correspondence: yossibug@ekmd.huji.ac.il
http://dx.doi.org/10.1016/j.stem.2015.08.006

SUMMARY

Induced pluripotent stem cells (iPSCs) undergo extensive nuclear reprogramming and are generally indistinguishable from embryonic stem cells (ESCs) in their functional capacity and transcriptome and DNA methylation profiles. However, direct conversion of cells from one lineage to another often yields incompletely reprogrammed, functionally compromised cells, raising the question of whether pluripotency is required to achieve a high degree of nuclear reprogramming. Here, we show that transient expression of Gata3, Eomes, and Tfap2c in mouse fibroblasts induces stable, transgene-independent trophoblast stem-like cells (iTSCs). iTSCs possess transcriptional profiles highly similar to blastocyst-derived TSCs, with comparable methylation and H3K27ac patterns and genome-wide H2A.X deposition. iTSCs generate trophoectodermal lineages upon differentiation, form hemorrhagic lesions, and contribute to developing placentas in chimera assays, indicating a high degree of nuclear reprogramming, with no evidence of passage through a transient pluripotent state. Together, these data demonstrate that extensive nuclear reprogramming can be achieved independently of pluripotency.

INTRODUCTION

The introduction of four transcription factors, Oct4, Sox2, Klf4, and Myc (OSKM) into somatic cells can initiate a reprogramming process that eventually yields stable and fully functional embryonic stem-like cells (also termed induced pluripotent stem cells [iPSCs]) (Takahashi and Yamanaka, 2006). The notion that as little as four factors are sufficient to reset the epigenome of a cell opened a new avenue where scientists have attempted to convert different adult cells into other somatic cell types by avoiding the pluripotent state using specific key master regulators. Cell types such as hematopoietic cells, different neuronal cells, cardiomyocytes, hepatocytes, embryonic Sertoli cells, endothelial cells, β cells, and pigment cells were converted from different somatic cells by employing the direct conversion approach (Lee and Young, 2013; Xu et al., 2015).

However, in contrast to iPSCs that are stable and closely resemble embryonic stem cells (ESCs) in their methylome, transcriptome, and function (Buganim et al., 2014), many of the directly converted cells are unstable (i.e., the cells are dependent either fully or partially on their exogenous factors) and represent only a partially reprogrammed state as estimated by their transcriptional profile and function (Cahan et al., 2014; Morris et al., 2014; Xu et al., 2015). This raises the question of whether a high degree of nuclear reprogramming is a unique property of cells undergoing reprogramming to pluripotency.

Trophoblast Stem Cells

In mammals, specialized cell types of the placenta mediate the physiological exchange between the fetus and mother during pregnancy. The precursors of these differentiated cells are trophoblast stem cells (TSCs). In the pre-implantation embryo, trophoblast cells are the first differentiated cells that can be distinguished from the pluripotent inner cell mass and form the outermost layer of the blastocyst (Cockburn and Rossant, 2010). In the mouse, TSCs can be isolated and cultured from outgrowths of either the blastocyst polar trophectoderm (TE) or extraembryonic ectoderm (ExE), which originates from the polar TE after implantation (Tanaka et al., 1998). The trophoblast cell lineage is the source for the most essential cell types of the placenta. Therefore, TSCs have tremendous biomedical relevance, as one-third of all human pregnancies are affected by placental-related disorders (James et al., 2014).

Here, we demonstrate that transient ectopic expression of three TSC key master regulators, Gata3, Eomes, and Tfap2c together with Myc in fibroblasts, initiates a mesenchymal-to-epithelial transition process that leads to the formation of a small number of stable and transgene-independent-induced TSCs (iTSCs) that resemble blastocyst-derived TSCs (bdTSCs) in their transcriptome, epigenome, and function. iTSCs differentiated

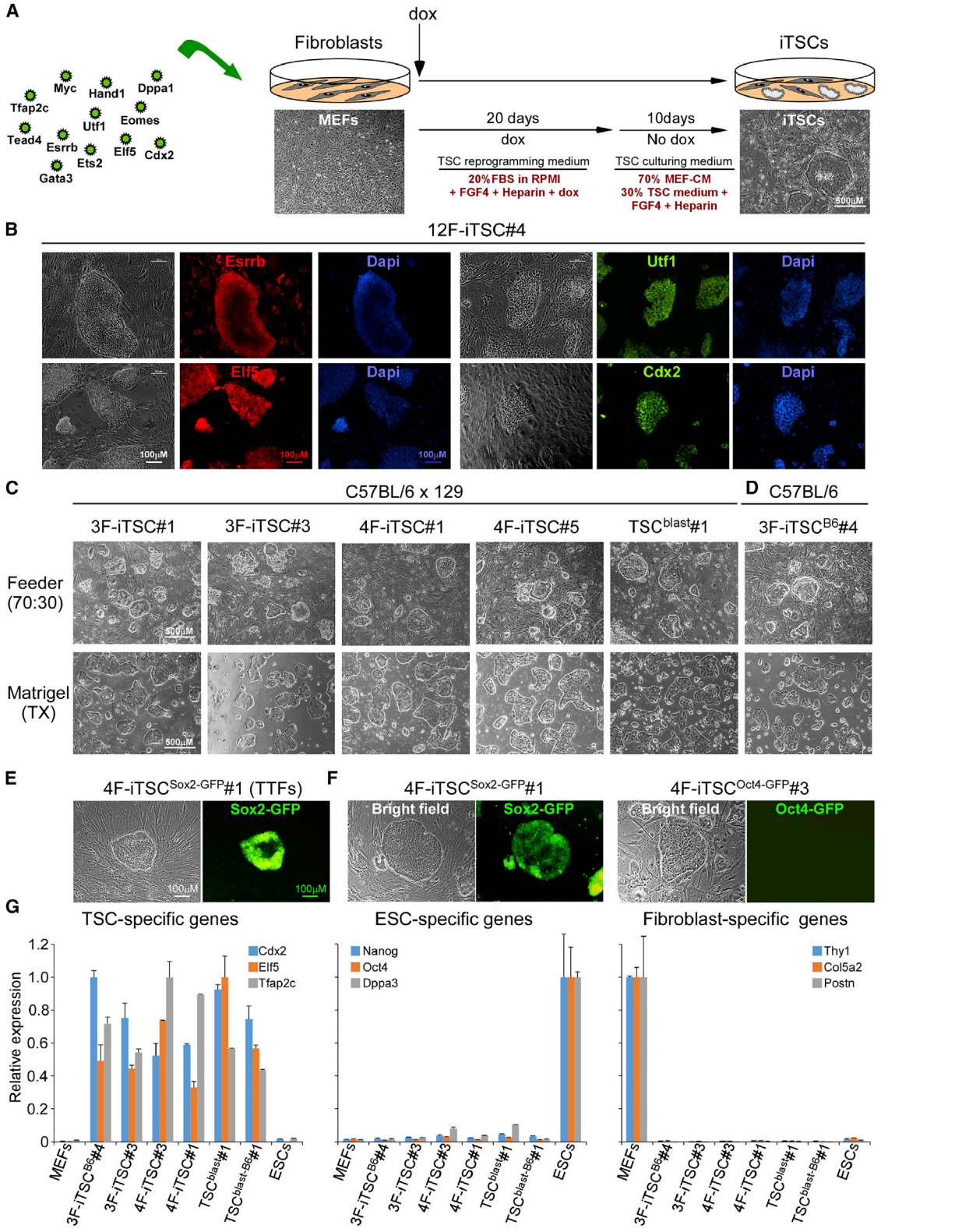

Figure 1. Gata3, Eomes, and Tfap2C Are Sufficient to Induce Reprogramming of MEFs into TSC-like Colonies

(A) Schematic representation of the strategy to reprogram MEFs into iTSCs. MEFs were infected with the depicted dox-inducible lenti-viral vectors. Infected MEFs were cultured in TSC reprogramming medium, containing dox for 20 days. Following 20 days of reprogramming, medium was replaced to TSC culturing medium. Ten days after, epithelial colonies with TSC-like morphology were isolated and cultured on feeder cells.

(legend continued on next page)

into all derivatives of the trophectoderm lineage in vitro, gave rise to hemorrhagic lesions in nude mice, and chimerized the placenta of the developing embryo, suggesting that iTSCs acquired all hallmarks of native TSCs.

RESULTS

Ectopic Expression of Gata3, Eomes, and Tfap2c Generates Stable Colonies that Are Similar in Their Morphology and Gene Expression to Trophoblast Stem Cells

We hypothesized that key master regulators that control early embryonic development should possess nuclear reprogramming capability, similarly to those expressed in pluripotent cells. To test this hypothesis, we decided to convert fibroblasts into trophoblast stem-like cells, which are the embryonic precursors of the placenta and thus are restricted only to one layer.

To generate induced trophoblast stem cells (iTSCs), we screened for transcription factors with a known role in trophoblast development and in reprogramming at large (Latos and Hemberger, 2014; Niwa et al., 2005; Ralston et al., 2010; Russ et al., 2000). Twelve transcription factors (12F): Tfap2c, Tead4, Hand1, Dppa1, Gata3, Ets2, Elf5, Cdx2, Eomes, Myc, Utf1, and Esrrb were cloned into doxycycline (dox)-inducible lentiviral vectors and then used to infect mouse embryonic fibroblasts (MEFs). To initiate the conversion process and select for stable clones (i.e., colonies that can grow and maintain their characteristics for prolonged culture time without exogenous factors), we exposed the cells to dox for 20 days and then removed dox for another 10 days (Figure 1A; for details see the Experimental Procedures). Ten days post dox withdrawal, epithelial colonies with TSC-like morphology developed in the dish (Figure 1A). We isolated five 12F-iTSC clones for further characterization. All isolated clones grew on mitomycin-c-treated MEFs, and similarly to freshly isolated blastocyst-derived TSCs (bdTSCs), could be weaned from feeder cells after five to ten passages. To examine whether the cells activated their endogenous TSC circuitry, we measured the mRNA and protein levels of several well-known TSC markers. As can be seen in Figure S1A, all clones expressed high endogenous mRNA levels of the TSC markers: *Elf5*, *Cdx2*, *Esrrb*, *Utf1*, *Tead4*, and *Hand1* (Figure S1A) and a high protein level of Esrrb, Utf1, Cdx2, and Elf5 (Figure 1B, representative clone is presented). To identify the minimum number of transcription factors that are required for generating iTSCs, we analyzed the five 12F-iTSC clones for their transgene integrations by qPCR. Surprisingly, although Cdx2 has been shown to be essential for determining TSC fate by counteracting pluripotency via the repression of Oct4 (Niwa et al., 2005; Strumpf et al., 2005), the only factors that were present in all five clones were Gata3, Eomes, and Tfap2c (Figure S1B). In accordance with that, expression of Gata3, Eomes, and Tfap2c (GET or 3F) was sufficient to generate iTSC clones (Figure 1C, two isolated stable clones are presented, upper panel). It is important to note that two of the 12 factors, Ets2 and Tead4, were present in four out of the five examined clones (Figure S1B), suggesting these factors have a positive effect on the reprogramming process. Since Myc was shown to be a global gene amplifier (Lin et al., 2012; Nie et al., 2012; Soufi et al., 2012), we tested whether ectopic expression of Gata3, Eomes, Tfap2c, and Myc (GETM or 4F) enables the formation of iTSCs (Figures 1C, two isolated stable clones are presented, upper panel, and S1C). To measure reprogramming efficiency, MEFs harboring a GFP reporter in the endogenous locus of the TSC/ESC marker Sox2 (Adachi et al., 2013), were infected with either GET or GETM. While GET produced an average of 112 Sox2-GFP-positive colonies per 3×10^5 seeded cells, GETM produced ~2-fold more Sox2-GFP-positive colonies (an average of 196 colonies, Figures S1D). Since more cells could initiate proliferation following Myc addition (Figure S1E), we believe that one of its main effects in boosting the reprogramming to iTSCs is by overcoming contact inhibition and senescence.

All isolated clones from GET (3F) and GETM (4F) grew for several passages under standard TSC culture conditions and could be weaned from feeder cells after five to ten passages. In addition, the clones could also be maintained under recently published defined medium and culture conditions (Kubaczka et al., 2014) (Figure 1C, lower panel) and exhibited a correct composition of transgenes in their genome (Figure S1F) with non-leaky or minor leaky expression of the transgenes (Figure S1G). iTSC clones were also generated from inbred strains such as C57BL/6 (Figure 1D) and adult tail-tip fibroblasts (TTFs) expressing Sox2-GFP, but with reduced efficiency (Figures 1E and S1D). Importantly, while the Sox2-GFP reporter was highly activated in iTSCs, the pluripotent reporter Oct4-GFP remained silent (Figures 1E and 1F). Fluorescence-activated cell sorting (FACS) analysis of Sox2-GFP-positive cells on one representative Sox2-GFP 4F-iTSC clone that grew either on feeder under standard TSC culture conditions or on Matrigel under defined culture conditions revealed a highly homogenous expression of Sox2 (83.4% and 98.9%, respectively, Figure S1H). Expression of the TSC-specific genes, *Cdx2*, *Elf5*, *Tfap2c*, *Ets2*, *Tead4*, and *Eomes* was comparable between various iTSC clones and two bdTSC lines, TSC^{blast}#1 and $TSC^{blast\text{-}B6}$#1, (Figures 1G and S1I). Moreover, the expression

(B) Bright field images and immunostaining against Esrrb, Utf1, Elf5, and Cdx2 in stable iTSC clone generated by 12 factors (12F). Scale bar, 100 μM.

(C) Bright field images of stable iTSC clones generated by three factors (3F, GET) and four factors (4F, GETM) and of bdTSC clone, TSC^{blast}#1, all from mice with mixed C57BL/6 × 129 background. Top: shows clones that grew under standard TSC culture conditions: 70% MEF conditioned medium (MEF-CM), 30% TSC medium +FGF4 (25 ng/ml), and heparin (1 μg/ml). Bottom: shows colonies that grew under defined culture condition: TX medium +FGF4 (25 ng/ml), heparin (1 μg/ml), and Tgfβ1 (2 ng/ml) on Matrigel.

(D) Bright field images of a stable iTSC colony generated by 3F from MEFs isolated from C57BL/6 mice.

(E) A stable iTSC colony expressing endogenous Sox2-GFP, generated by 4F from Sox2-GFP tail-tip fibroblasts (TTFs). Cells were imaged using the bright field and GFP channel.

(F) Left: a stable iTSC colony generated by 4F from Sox2-GFP MEFs expressing endogenous Sox2-GFP. Right: a stable iTSC colony generated from Oct4-GFP MEFs shows lack of Oct4-GFP expression. Cells were imaged using the bright field and GFP channel.

(G) qPCR of the indicated genes normalized to *Gapdh* in MEFs, 3 and 4 factors representative iTSC clones, bdTSC clones, and ESCs.

See also Figure S1.

of the pluripotent-specific genes, *Nanog*, *Oct4*, and *Dppa3*, and the expression of the fibroblast-specific genes, *Thy1*, *Col5a2*, and *Postn* was absent in all examined iTSC clones and bdTSCs (Figure 1G). In total, we isolated and cultured 18 3F-iTSC clones and 24 4F-iTSC clones with *isolation efficiency* of ~50% of Sox2-GFP-positive colonies becoming stable iTSC clones. The results so far suggest that the introduction of Gata3, Eomes, and Tfap2c into somatic cells generates stable colonies that can be maintained in culture independently of their exogenous factors and are similar in their morphology and TSC-specific marker expression to bdTSCs.

Introduction of Gata3, Eomes, Tfap2c, and Myc into Fibroblasts Induces Rapid Mesenchymal-to-Epithelial Transition

Mesenchymal-to-epithelial transition (MET) is an essential process for proper embryonic development and is initiated early on during the conversion of fibroblasts into epithelial cells such as iPSCs and Sertoli cells (Buganim et al., 2012a, 2012b). Since TSCs are epithelial cells, we sought to examine at what time point during the conversion the induced fibroblasts undergo MET. First, we monitored the morphology of the induced cells for 8 days following GET expression alone or in combination with Myc. To clearly observe the morphology of the induced cells overtime, we plated the cells at low density. As can be seen in Figure 2A, a morphological change can already be observed after 2 days of GETM expression. On day 8, a large number of epithelial colonies developed in the plate due to increased proliferation, suggesting that MET is an early event in the reprogramming process to iTSCs with GETM. In contrast, when fibroblasts were infected with GET alone, fewer colonies developed in the plate, and clear epithelial colonies could be seen only on day 12 of dox exposure, suggesting a less prominent MET process (Figure 2B). To investigate how GETM initiate MET, we monitored the mRNA levels of several key genes that were shown to play a major role in the opposite process, epithelial-to-mesenchymal transition ((EMT) (Figure 2C). A substantial downregulation of key EMT genes such as *Twist1*, *Zeb2*, *Snai2*, *Foxc2*, *Gsc*, *Mmp3*, and *Snai1* was noted after 2 days of factor induction and remained low for the first 8 days (Figures 2D and S2A). Consequently, a sharp decrease was observed in mesenchymal markers such as *Cdh2*, *Des*, *Fn1*, and *Cldn1* and a gradual elevation in epithelial markers such as *Cdh1*, *Krt18*, *Dsp*, and *Ocln* (Figures 2E, 2F, S2B, and S2C). The same trend was observed with GET but to a much lesser extent (Figure S2D), suggesting that Myc contributes to the induction of the MET process. This is in agreement with a previous study demonstrating that Myc alone is sufficient to downregulate mesenchymal markers (Sridharan et al., 2009). Upregulation of the epithelial markers Krt18 and Cdh1, and downregulation of the mesenchymal marker Acta2, were also observed at the protein level (Figure 2G). Interestingly, the expression levels of the epithelial markers *Krt18* and *Ocln*, and the mesenchymal markers *Twist1*, *Zeb2*, *Cdh2*, and *Snai1*, were similar between TSCs and induced cells and different from ESCs. These results suggest that MET is an early and robust phenomenon occurring during the conversion to iTSCs and that expression of GET or GETM in mesenchymal cells induces epithelial morphology with characteristics resembling those of bdTSCs.

iTSCs Exhibit Similar Transcriptome and Karyotype to Those of bdTSCs

One indication for a stable conversion and a high degree of nuclear reprogramming state is the capability of the induced cells to activate their endogenous circuitry (Buganim et al., 2013). Incomplete activation of the endogenous circuitry will lead to a partially similar transcriptional profile, as can be seen in many direct conversion models (Cahan et al., 2014; Morris et al., 2014). To assess whether isolated iTSCs activate their endogenous circuitry, we subjected two 12F-iTSC clones, two 4F-iTSC clones, and two 3F-iTSC clones for RNA-sequencing (RNA-seq) analysis. Two bdTSC clones and parental MEFs and ESCs were used as positive and negative controls, respectively. Notably, the various iTSC clones clustered together with bdTSC clones and far away from the MEF and ESC controls, as indicated by hierarchical clustering analysis (Figure 3A). Importantly, one of the bdTSC lines, TSC^{blast}#1, clustered closer to the three induced TSC clones, 4F-iTSC#1, 3F-iTSC#3, and 3F-iTSC#4, than to the other bdTSC line, $TSC^{blast\text{-}B6}$#1 (Figure 3A). Principle component analysis (PCA) (Figure 3B), scatter plots (Figure 3C), and an unbiased clustering heatmap of the top 10,000 expressed genes (Figure S3A) confirmed the results obtained by hierarchical clustering and demonstrated a highly similar transcriptome between bdTSCs and iTSCs.

Stress induced by oncogenes such as Myc leads to DNA damage that promotes genomic instability and tumor progression. Thus, we asked whether iTSCs acquire genomic aberrations in the course of the reprogramming process. To this end, we examined the chromosomal content of iTSC clones by whole genome single-cell sequencing and compared it to bdTSCs, MEF, and ESC controls. Single-cell sequencing libraries were made from nine cell lines (ESCs, parental MEFs, three 3F-iTSC, two 4F-iTSC, and two bdTSC clones) that were cultured for at least 20 passages. Notably, although a larger number of chromosomal aberrations was noticed in all TSC lines compared to ESC and MEF controls, the iTSC clones exhibited a comparable extent of abnormal chromosomal content to the two bdTSC lines, suggesting that the reprogramming process per se, did not lead to an increased number of genomic aberrations (Figure S3B). We also mapped sister chromatid exchanges (SCEs), a sensitive indicator of genomic stress, in seven lines using Strand-seq (Falconer et al., 2012). Analysis of average SCE rates in all lines showed no significant differences between any of the cell types (Figure S3C, representative library is present in Figure S3D). The results so far suggest that iTSCs resemble bdTSCs in their transcriptome and genomic stability.

iTSCs Exhibit Comparable Methylation and Epigenome Patterns and H2A.X Deposition to bdTSCs

A high level of nuclear resetting refers to the remodeling of a new epigenome that is similar to the corresponding cell type. To test whether iTSCs acquired epigenetic marks that are specific to TSCs, we measured the DNA methylation status of one TSC-specific locus (i.e., a locus that is hypomethylated in TSCs but hypermethylated in MEFs and ESCs), the *Elf5* promoter, and one ESC-specific locus, the *Nanog* promoter, in two iTSC clones, two bdTSC clones, and the parental MEFs and ESCs by bisulfite conversion and sequencing. As can be seen in Figure 4A, while the *Elf5* promoter exhibited robust

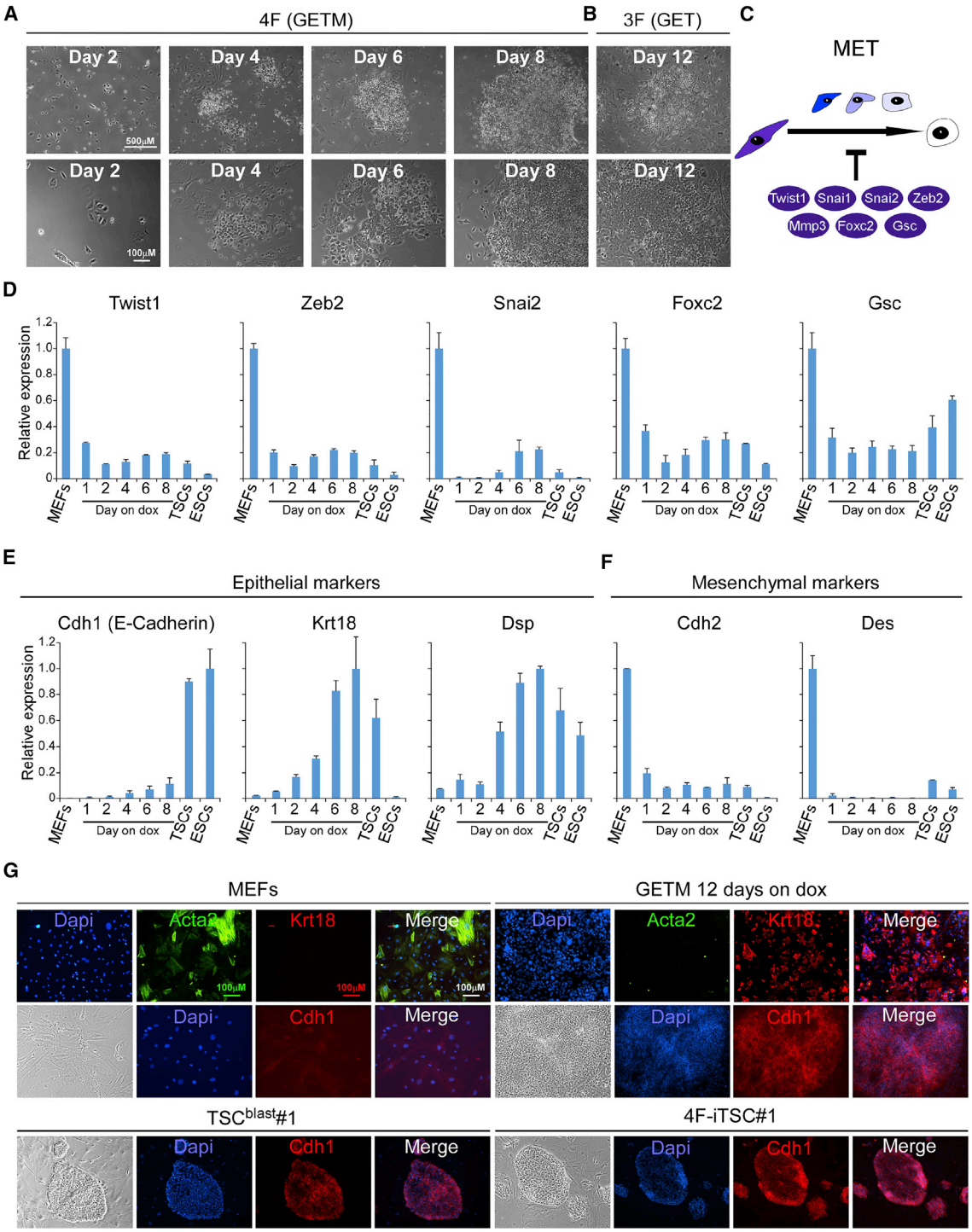

Figure 2. Reprogramming to iTSCs Begins with the Initiation of a Mesenchymal-to-Epithelial Transition

(A and B) Representative bright field images showing the formation of epithelial foci within the indicated days of iTSC reprogramming with GETM (A) or GET (B).

(C) Schematic representation of the mesenchymal-to-epithelial transition (MET) process and key factors that block it (modified from Buganim et al., 2012b).

(D–F) qPCR of the indicated genes, normalized to *Gapdh* in MEFs, MEFs on dox for the indicated amount of days, bdTSCs, and ESCs.

(G) Representative immunostaining images depicting the protein levels of the epithelial markers Krt18 and Cdh1 and the mesenchymal marker Acta2 in cells ectopically expressing GETM for 12 days. Lower panel: immunostaining images depicting the protein levels of Cdh1 in bdTSCs and in the 4F-iTSC#1 clone.

See also Figure S2.

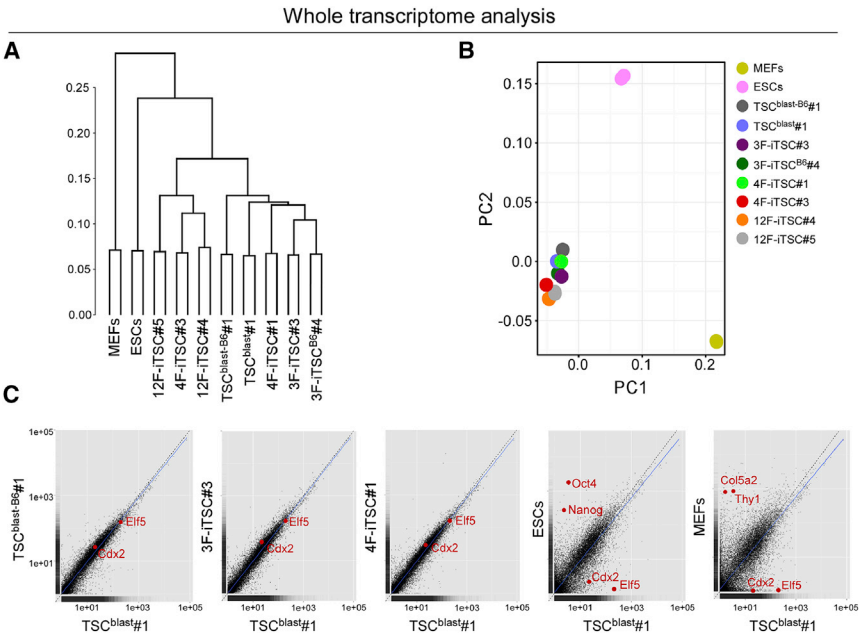

Figure 3. Unbiased Comparative Transcriptome Analyses Clusters iTSCs with bdTSCs and Far from ESCs or MEFs

(A) Hierarchical clustering of global gene expression profiles for two RNA-seq technical replicates for the indicated iTSC, bdTSC, ESC, and MEF lines. Replicate pairs were assigned a shared numerical value.

(B) Principle component analysis for genes from (A). PC1, 27%; PC2, 19%. Each of the iTSC, bdTSC, ESC, and MEF lines is marked by a specific color. The group names correspond to the names in (A).

(C) Scatter plots for the indicated comparisons. Blue line shows the linear representation of the data, black line shows the y = x line. Red dots show the position of the indicated genes. All examined TSC and iTSC clones grew under defined TX medium. See also Figure S3 and Table S1.

hypomethylation in all examined iTSC and bdTSC clones, it remained hypermethylated in ESC and MEF controls (Figure 4A). In contrast, the *Nanog* promoter was hypomethylated only in the ESC control sample.

Several loci have been suggested to act as gatekeepers in the transdifferentiation of mouse ESCs to TSC-like cells upon manipulation of lineage-determining transcription factors such as Cdx2 and Oct4 (Cambuli et al., 2014). These regions exhibited a higher methylation status and lower gene expression in all transdifferentiation models as compared to bdTSCs. Thus, we examined the expression level of these gatekeeper genes in various iTSC clones. As can be seen in Figure 4C, although some variation in gene expression was noticed in a number of genes, the overall gene expression was comparable between iTSC clones and the two bdTSCs (Figure 4C). Methylation analysis of one representative locus, the *Hand1* promoter, revealed a robust hypomethylation in bdTSC and iTSC lines compared to MEF control (Figure S4A). Interestingly, hypomethylation was also observed in ESC, suggesting that the *Hand1* promoter region (−110 to +40) is not ideal for discriminating between the methylation status of ESC and TSCs.

The histone mark H3K27ac identifies accessible chromatin throughout the genome and can separate active from poised enhancers (Creyghton et al., 2010). Thus, we tested whether TSC-specific regions are more enriched with H3K27ac in bdTSCs and iTSCs than in MEF and ESC controls. In agreement with their capability to express the *Cdx2* and *Hand1* genes, to repress the fibroblast *Thy1* and *Postn* genes, and to retain low levels of the ESC genes *Nanog* and *Oct4*, bdTSCs and iTSCs showed high H3K27ac levels only for the *Cdx2 and Hand1* loci while retaining low H3K27ac levels for *Nanog*, *Oct4*, *Thy1*, and *Postn* following chromatin immunoprecipitation (ChIP)-qPCR analysis (Figure S4B). The results so far indicate that the epigenome of iTSCs was rewired to be equivalent to that of bdTSCs, as assessed by methylation and H3K27ac enrichment of specific loci, and suggests an explanation for the low expression of the *Hand1* gene in ESCs, although hypomethylated in its promoter region (Figure S3A).

Genome-wide organization of histone variant H2A.X is cell type dependent. Abnormal H2A.X deposition is frequently observed in iPSC clones generated by OSKM factors that failed to support "all-iPSC" mice development (Wu et al., 2014). In contrast, iPSCs that are generated with other reprogramming factors, such as, Sall4, Nanog, Esrrb, and Lin28 (SNEL), mostly support the development of "all-iPSC" mice and show normal H2A.X deposition (Buganim et al., 2014). We thus examined the genome-wide H2A.X deposition patterns of two 3F-iTSC, two 4F-iTSC, and two bdTSC clones and compared them to ESC and MEF controls, using chromatin immunoprecipitation sequencing (ChIP-seq). H2A.X deposition patterns in all examined iTSC clones closely resembled bdTSC clones and were significantly different ($p < 1.0E-100$) from MEF and ESC controls (Figure 4D, the deposition patterns of H2A.X in four different chromosomes are presented in Figures 4E and S4C). These data suggest that iTSCs have acquired key epigenetic landscape signatures of TSCs during the conversion process.

iTSCs Function Similarly to bdTSCs

Cells acquiring a high degree of reprogramming state should exhibit all the functions of their corresponding cells, as can be seen in the case of high quality iPSCs and ESCs. To test whether iTSCs are capable of executing the functions exerted by bdTSCs, we subjected them to three gold-standard tests. First, we examined whether iTSCs are multipotent and capable of differentiating into trophoblast lineages represented in the placenta. iTSCs were cultured on gelatin without Fgf4 and heparin for 10 days and, after 2 days, differentiated giant multinucleated cells, associated with primary trophoblast cells, were noted in the plate (Figure 5A, second image from the left). The presence of multinucleated cells and their growing number over the differentiation period was evident also by flow cytometry analysis with propidium iodide (PI) (Figure 5B). Accordingly, we observed a gradual elevation in gene expression of the

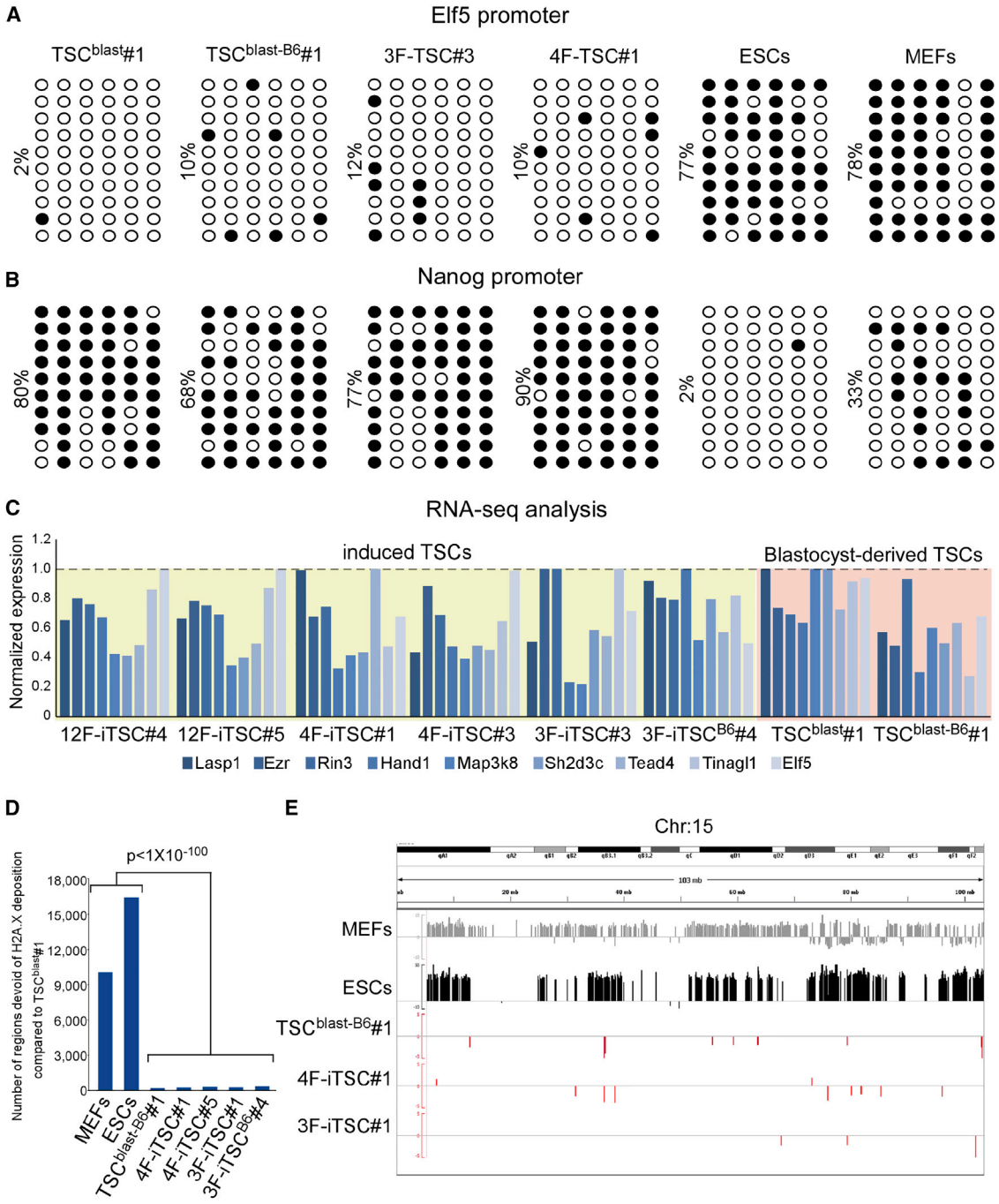

Figure 4. Promoter Methylation Analysis of *Elf5* and *Nanog* and H2A.X Deposition Demonstrate High Similarity between iTSCs and bdTSCs

(A and B) Bisulfite analysis of the promoter regions of *Elf5* (−652 to −263) and *Nanog* (−399 to +49) in bdTSCs, iTSCs, ESCs, and MEFs. Each circle (empty-hypomethylated and full hypermethylated) represents one CG sequence in the depicted locus and each row represents one PCR product that was cloned into TA cloning vector and sequenced.

(C) A graph summarizing the expression levels of the indicated gatekeeper genes in the indicated samples as measured by RNA-sequencing.

(D) A bar chart summarizing the number of differential H2A.X deposition domains (compared to TSC^{blast}#1 control line) in the indicated iTSC and bdTSC lines, MEFs and ESCs (p value < 1.0E-100, chi-square test).

(E) Comparative H2A.X depositions in the indicated iTSC clones, bdTSCs, ESCs, and MEFs at chromosome 15 (Chr15). y axis: relative H2A.X deposition level (RSEG enrichment score, compared to bdTSC control line, see Supplemental Experimental Procedures). Positive value: regions enriched for H2A.X deposition over control; negative values: regions devoid of H2A.X deposition over control.

See also Figure S4 and Table S1.

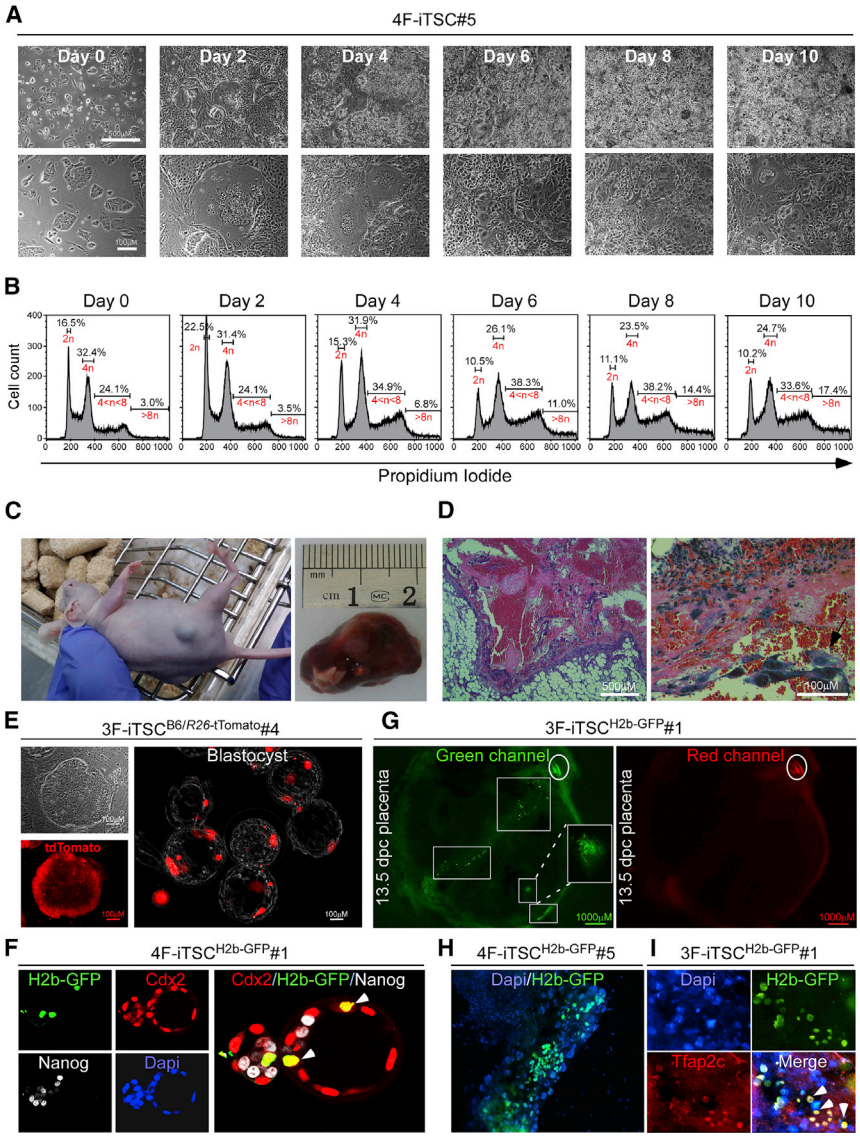

Figure 5. iTSCs Are Fully Functional

(A) Bright field images of iTSCs grown in differentiation medium (10% FBS DMEM medium without Fgf4 and heparin) for the indicated days.

(B) Flow cytometry analysis of iTSCs grown in differentiation medium for the indicated days following propidium iodide (PI) staining. Gates show PI staining intensities, indicating DNA copy number. The percentage of cells from each sample in every phase is indicated. PI was measured with filter Fl3.

(C) A representative hemorrhagic lesion, 7 days after subcutaneous injection of iTSCs (5×10^6) into a nude mouse.

(D) H&E staining of paraffin sections of hemorrhagic lesions. Left: low power image. Right: higher power image showing necrotic tissue with blood and scattered giant cells (arrow).

(E) Left: a stable iTSC colony, 3F-iTSC$^{B6/R26\text{-tdTomato}}$#4, with constitutive tdTomato expression from the *Rosa26* locus. Cells were imaged using the bright field and red channel. Right: 3F-iTSC$^{B6/R26\text{-tdTomato}}$#4 cells were injected into 8-cell stage embryos and analyzed at the hatched blastocyst stage using fluorescent microscopy.

(F) 4F-iTSC$^{H2b\text{-}GFP}$#1 cells were injected into 8-cell stage embryos and analyzed at the hatched blastocyst stage using confocal fluorescent microscopy. Blastocysts were stained for Cdx2 (red) to detect trophectoderm cells, and for Nanog (white) to detect cells from the inner cell mass. Co-localization of H2b-GFP nuclei and Cdx2 nuclei is depicted by white arrows (yellow staining).

(G) Contribution of H2b-GFP iTSCs, 3F-iTSC$^{H2b\text{-}GFP}$#1, to the developing 13.5 dpc placenta. A clear H2b-GFP signal was detected in several patches within the placenta (white squares) and was completely absent in the embryo. Placentas were imaged using green and red channels to detect autofluorescence. A magnification of one region is illustrated by dashed lines. White oval shows autofluorescent structure.

(H) Immunostaining of GFP in placental tissue isolated from E13.5 fetus following blastocyst injection of 4F-iTSC$^{H2b\text{-}GFP}$#5 cells shows nuclear GFP staining.

(I) Immunostaining of GFP and Tfap2c in placental tissue isolated from E13.5 fetus following blastocyst injection of 3F-iTSC$^{H2b\text{-}GFP}$#1 cells shows double positive yellow cells (white arrows).

See also Figure S5 and Table S1.

specific trophoblast giant cell markers *Ctsq*, *Prl3b1*, *Prl3d1*, and *Prl2c2* (Simmons et al., 2007) in two iTSC clones and one bdTSC clone following differentiation (Figure S5A). Other trophoblast-lineage markers such as *Tpbpa* (specific for spongiotrophoblast cells) (Simmons and Cross, 2005) and *Cga* (specific for syncytiotrophoblast cells) (Anson-Cartwright et al., 2000) were elevated as well, and undifferentiated TSC markers such as *Cdx2* and *Eomes* (Ng et al., 2008) were downregulated during differentiation (Figure S5A).

The formation of a transient hemorrhagic lesion under the skin of a nude mouse by transplanted bdTSCs recapitulates the invading properties of the trophoblast giant cells during implantation (Kibschull et al., 2004). Similar to bdTSCs, when injected subcutaneously into nude mice, iTSCs formed lesions that reached their maximum size 5–8 days following injection and thereafter began to resorb (Figure 5C). Some of the lesions were excised and analyzed by H&E staining, revealing a typical structure of trophoblastic hemorrhagic lesion with big blood-filled lacunas and differentiated trophoblastic giant cells (Figure 5D). Next, we tested whether iTSCs can function properly in their native environment. First, we injected tdTomato-iTSCs into 8-cell stage embryos and followed the localization of the injected cells at the blastocyst stage. Notably, the vast majority of the cells migrated toward the outer layer of the blastocysts in accordance with their role as extraembryonic cells (Figure 5E). To accurately localize the cells inside the blastocyst we infected iTSCs with H2b-GFP lentiviral vector to better visualize the nuclei of the cells (Figure S5B). H2b-GFP marked iTSCs were injected

into eight-cell-stage embryos that were cultured until the blastocyst stage. The blastocysts were then fixed and stained for Cdx2 and Nanog and analyzed by confocal fluorescent microscopy. As can be seen in Figure 5F, the injected H2b-GFP iTSCs were negative for Nanog, positive for Cdx2, and localized to the extra-embryonic region similarly to bdTSCs (Figures 5F and S5C, left panel). Importantly, many of the injected H2b-GFP-positive bdTSCs or iTSCs lose the expression of Cdx2 during blastocyst maturation (Figure S5C, right panel), proposing an explanation for the low contribution efficiency of bdTSCs to developing placenta seen following blastocyst injection (Cambuli et al., 2014). Moreover, this observation suggests an active mechanism inside the blastocyst to shot off any cell that is wrongly localized in the blastocyst.

It has been shown that bdTSCs can contribute to the formation of the placenta when injected into blastocysts (Niwa et al., 2005; Tanaka et al., 1998). Thus, we asked whether iTSCs could chimerize the developing placenta as well. Examination of 13.5 days post-coitum (dpc) placentas by fluorescent microscope revealed many structures with high autofluorescence activity both in the green and red channels. We therefor used again H2b-GFP iTSCs, as nuclear GFP signal is unique and can be easily distinguished from other structures of the placenta. Marked clones were injected into blastocysts that were then transferred into pseudopregnant females. On 13.5 dpc, placentas and embryos were isolated and analyzed. A clear H2b-GFP signal was detected in some placentas (an average of 2 out of 15 examined placentas) in several patches and was completely absent from all embryos (representative patches of nuclear-GFP cells are depicted in Figures 5G, 5H, S5D, and S5E). To examine whether the cells differentiated into the trophoblast lineage, we stained the placenta with Tfap2c antibody. As can be seen in Figure 5I, double-positive cells for H2b-GFP (green) and Tfap2c (red) were detected in 13.5 dpc placentas (Figure 5I). Importantly, a comparable contribution was seen following the injection of a bdTSC line, $TSC^{blast\text{-}H2b\text{-}GFP}$#1 (data not shown). These data suggest that iTSCs are fully functional cells with the capability to recapitulate the tasks exerted by bdTSCs.

The Conversion of Fibroblasts into iTSCs Does Not Occur via a Defined Pluripotent State

Since ESCs and TSCs share the expression of several key genes (e.g., *Sox2*, *Sall4*, *Utf1*, *Esrrb*) (Figures 1B, S1A, and S6A), and because Gata3 was shown to induce pluripotency in other combinations of factors (Montserrat et al., 2013; Shu et al., 2013), we examined whether the conversion to iTSCs goes through a defined pluripotent stage. First, we tried to obtain iTSCs by ectopic expression of OSKM in cells that grew under culture conditions of TSCs. As a control, we cultured the cells also under ESC culture conditions. MEFs that harbor the Nanog-GFP or Oct4-GFP reporters were used because *Nanog* and *Oct4* are expressed solely and specifically in pluripotent cells (Figure 1G). Transduced MEFs were exposed to dox for 13 days, after which it was removed for 6 days. As can be seen in Figure 6A, we observed only differentiated cells (right panel) or stable iPSCs (left panel) that were also positive for the Nanog-GFP or Oct4-GFP reporters in the dish of both culture conditions (Figure 6A). The number of GFP-positive cells was drastically lower when TSC culture conditions were used, suggesting that reprogramming with TSC culture conditions is suboptimal for acquiring a stable pluripotent state (Figure 6A) and that the acquisition of a pluripotent state is not beneficial for the formation of iTSCs. Next, we tried to obtain iPSCs by using the TSC reprogramming factors, GETM. The cells were cultured either under standard ESC culture conditions (serum and LIF), or under optimal mouse ESC culture conditions (LIF and 2i, GSK3β and Mek 1/2 inhibitors) to facilitate pluripotency. We were unable to attain stable iPSCs in all examined conditions, even when the cells were exposed to dox for a longer period of time (data not shown). We next asked whether Nanog or Oct4 are activated during the reprogramming process to iTSCs. The presence of Nanog-GFP- or Oct4-GFP-positive cells during the reprogramming process might suggest that these cells acquire a short and transient pluripotent state. To this end, we repeated the above experiments, but this time we analyzed the reprogrammable cells every 3 days by flow cytometry. Figure S6B shows that, in general, GFP-positive cells were undetectable during the 12 days of the reprogramming process. In some rare cases, we did observe a very small number of GFP-positive cells, but since multiple attempts to culture these cells (following sorting), either under TSC or ESC culture conditions, never gave rise to any growing cells, we believe this observation was either due to a high autofluorescent activity of dead cells in the green channel or as a results of an aberrant activation of the *Nanog* or *Oct4* locus (Figure S6B). Supporting this is the observation that even an early and robust marker for pluripotency such as *Fbxo15* was not activated following GETM induction (Figure S6C). In addition, iTSC colonies could be obtained when JAK inhibitor (JAKi), that blocks Stat3 phosphorylation, was added to the reprogramming medium (Figure S6D), and even when we looped out *Oct4* from the starting MEFs (i.e., Sox2-GFP MEFs harboring Oct4 lox/lox homozygous alleles) (Kehler et al., 2004) using a lentiviral vector encoding for Cre (Figure 6C). To rule out the possibility that GETM induces a hyperdynamic chromatin state (Buganim et al., 2013) or transient pluripotency phase (Bar-Nur et al., 2015) similarly to OSKM, we repeated the protocol by Efe et al. (2011) for inducing cardiomyocytes from fibroblasts. Notably, while we obtained a large number of cardiomyocyte colonies when we used OSKM as reprogramming factors, we never detected cardiomyocyte colonies while employing the GETM reprogramming factors, even when the reprogramming factors were expressed for a longer period of time (Figures 6D and 6E). The OSKM-derived cardiomyocyte colonies were positive for the cardiomyocyte marker Tnnt2 and approximately half of them were beating (Figures 6E, 6F, and S6E; Movies S1 and S2). These results suggest that the GETM reprogramming factor combination is specific for the trophectoderm lineage and that iTSC formation does not go through a defined pluripotency phase.

DISCUSSION

To convert one cell type to another and to reach a high degree of nuclear reprogramming state, the key master regulators of the targeted cell type must first be identified and then ectopically expressed. To complete the conversion process and to achieve a stable and fully functional cells, the exogenous factors must be

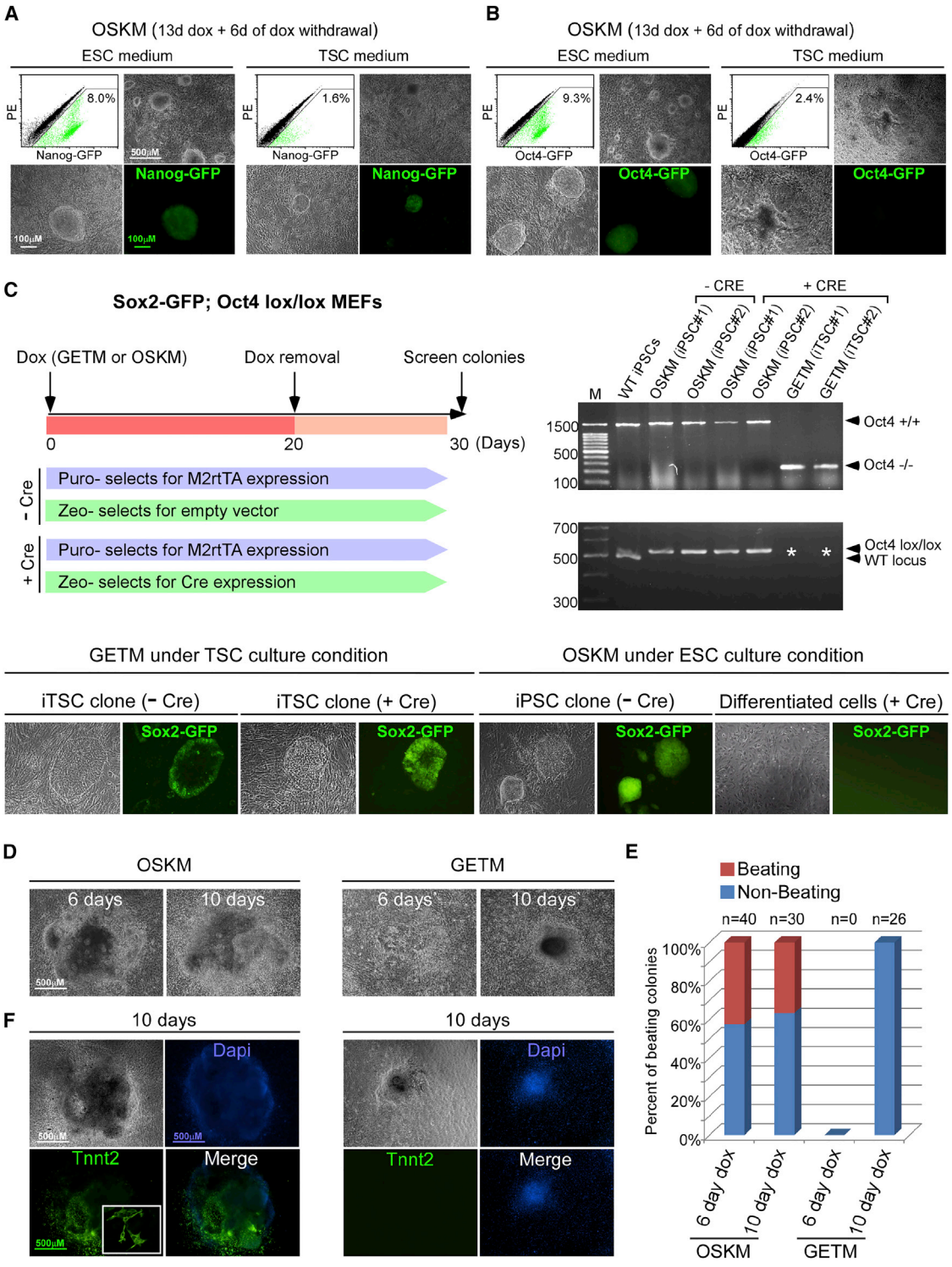

Figure 6. Reprogramming to iTSCs Occurs Directly via the Extraembryonic Lineage and Not via a Pluripotent State

(A and B) Bright field and green channel images and FACS analysis of iPSCs generated by OSKM expression in Nanog-GFP (A) or Oct4-GFP (B) MEFs grown in ESC or in TSC medium. Note that in the left panels a stable iPSC colony is presented and in the right panels differentiated cells under TSC culture conditions are presented.

(C) Upper left: schematic representation of strategy for inducing iTSC or iPSC clones without Oct4 presence. Two days prior to day 0, Sox2-GFP; Oct4 lox/lox MEFs (Kehler et al., 2004) were infected with dox-inducible GETM or with OSKM in combination with FUW-M2rtTA-2A-puro and FUW-Zeo-Cre or with FUW-Zeo-TetO empty vector. Starting on day 0, MEFs underwent 20 days of dox treatment, followed by 10 days without dox. Puromycin and Zeocin were added during the

(legend continued on next page)

downregulated, either by the cells (i.e., silencing) or by inducible systems.

Following the discovery of iPSCs, many other cell-type-specific key master regulators have been suggested to convert somatic cells by avoiding the pluripotent state. However, a high nuclear reprogramming state was evident only in iPSCs. This observation raised the hypothesis that complete nuclear resetting is a unique property for cells undergoing reprogramming to pluripotency. To test this hypothesis, we decided to convert fibroblasts into trophoblast stem-like cells. We chose TSCs because first, they are embryonic cells, and, in contrast to iPSCs, are committed only to one lineage, the trophectoderm. Second, key TSC master regulators such as Cdx2, Tead4, Eomes, Tfap2c, and Elf5 oppose the pluripotent state by repressing the core pluripotency circuitry, thus minimizing the possibility that the conversion to iTSC will go through a pluripotent state (Adachi et al., 2013; Chen et al., 2010; Niwa et al., 2005). Third, to date, all attempts to isolate and culture human TSCs in their undifferentiated state were unsuccessful (Genbacev et al., 2013). Identifying the combination of TSC key master regulators that can activate the TSC core circuitry in the murine model might aid in attaining the human undifferentiated state following expression of their human orthologs, as was shown recently to be the case for human naive-like ESCs by the transient ectopic expression of NANOG and KLF2 (Takashima et al., 2014; Theunissen et al., 2014). Fourth, recurrent miscarriage and fetal growth restriction (FGR) are associated with placental dysfunction and contribute to handicaps and in severe cases, fetal death. The generation of stable and fully functional human iTSCs will aid in modeling these diseases and, in the future, might provide a platform for cellular transplantation of intact and healthy iTSCs into undeveloped/damaged placenta (James et al., 2014).

It has been shown that ESCs can acquire trophoblast stem-like characteristics upon manipulation of lineage-determining transcription factors such as Cdx2, Elf5, Eomes, Tfap2c, Gata3, Oct4, or following activation of the extracellular signal-regulated kinase 1/2 (Erk1/2) pathway (Cambuli et al., 2014; Kuckenberg et al., 2010; Lu et al., 2008; Ng et al., 2008; Nishioka et al., 2009; Niwa et al., 2000, 2005; Ralston et al., 2010). Although transdifferentiation into trophoblast stem-like cells was initiated following these manipulations, lineage conversion remained incomplete in all models as evidenced by the failure to demethylate a small group of TSC genes such as *Elf5*, *Tead4*, and *Ezr* (Cambuli et al., 2014). Importantly, failure to demethylate this small group of loci was accompanied by reduced levels of their corresponding genes. Forced expression of the genes from these non-reprogrammed loci improved transdifferentiation efficiency, but still failed to confer a stable TSC phenotype (Cambuli et al., 2014). These data suggest that the optimal combination of factors that can completely activate the TSC core circuitry has not been identified to date.

Here, we describe a method to generate stable and fully functional TSC-like cells from murine fibroblasts by transient ectopic expression of three TSC key master regulators, Gata3, Eomes, and Tfap2c. Surprisingly, the two key TSC master regulators, Cdx2 and Elf5, were dispensable for the reprogramming process. The induced TSCs grew independently of the exogenous factors for a large number of passages and resembled bdTSCs in their morphology, transcriptome, methylation, and epigenetic status (as evident from several specific loci), H2A.X organization, and function (Table S1).

Whole transcriptome analyses demonstrated that the transcriptome of iTSCs is highly similar to bdTSCs, as one of the two bdTSC lines clustered closer to three iTSC clones than to the second bdTSC line. One of the loci that was relatively hypermethylated in all transdifferentiation models described above is the stringently regulated gatekeeper gene, *Elf5*. While 16% of this locus was methylated in bdTSCs, in the Oct4-downregulation transdifferentiation model and in the Cdx2 overexpression model, it was 26.5% and 64%, respectively (Cambuli et al., 2014). In the current study, measuring the methylation status of the *Elf5* promoter in two bdTSC lines (2% and 10%) and in two iTSC clones (10% and 12%) revealed robust and comparable hypomethylation. However, given the low efficiency of the reprogramming process, compared with the very high rate of transcription factor induced conversion of ESCs to TSCs, it is plausible to assume that there is a small population of cells present within ESC-derived TSC-like populations that is equivalent to bdTSCs. These data suggest that the conversion of fibroblasts into iTSCs represents a very high degree of nuclear reprogramming and refute the hypothesis that complete nuclear reprogramming can be achieved only in cells undergoing conversion to ESC-like cells. Similar to the initial studies in iPSCs, this method of conversion still needs fine-tuning and optimization such as identifying the ideal culture conditions and the best stoichiometry of the reprogramming factors.

entire course of the experiment. Clones from all plates were picked on day 30 and genomic DNA was purified. Upper right: semiquantitative PCR using primers for the recognition of Cre activity on *Oct4* loxP sites, as described previously (Kehler et al., 2004). Up: primer pair C, producing a 245 bp fragment from deleted alleles and a 1,421 or 1,455 bp fragment from WT or floxed alleles, respectively. Note that we could isolate only iTSC colonies with *Oct4* deleted alleles, although the overall number of colonies was reduced compared to WT cells. The very few stable iPSC clones that emerged from the reprogramming process that contained the Cre plasmid, escaped recombination and did not deleted *Oct4* as indicated by a 1,455 PCR product. Bottom: primer pair A, producing a 498 bp fragment from *Oct4* WT alleles or a 532 bp fragment from *Oct4* floxed alleles or no PCR product (white asterisk) from *Oct4* deleted alleles. Lower panel: representative images of iTSC (left) and iPSC (right) colonies, with or without Cre expression.

(D) Direct reprogramming to cardiomyocytes. MEFs infected with dox-inducible OSKM or GETM factors were exposed to reprogramming media containing JAK inhibitor (JAKi) for 6 or 10 days, followed by 3 days of dox withdrawal. Cells were then differentiated to cardiomyocytes by a chemically defined medium supplemented with BMP4 for 5 days, followed by 7 days of BMP4 withdrawal. Bright field images of beating colonies generated by OSKM are seen on the left, while non-beating colonies generated by GETM are seen on the right.

(E) Graph summarizing the percentages of beating and non-beating colonies out of the total "n" number of colonies generated by OSKM or by GETM, 6 and 10 days following dox induction.

(F) Left: bright field images and immunostaining against Tnnt2 in a beating colony generated by OSKM, 10 days following dox induction. Right: bright field images and immunostaining against Tnnt2 in cells infected with GETM, 10 days following dox induction.

See also Figure S6 and Movies S1 and S2.

EXPERIMENTAL PROCEDURES

Cell Culture and Mice

Mouse embryonic fibroblasts (MEFs) and tail-tip fibroblasts (TTFs) were isolated as previously described (Wernig et al., 2008). MEFs and TTFs were grown in DMEM supplemented with 10% FBS, 2 mM L-glutamine, and antibiotics. ESCs and iPSCs were grown in DMEM supplemented with 15% FBS, 1% non-essential amino acids, 2 mM L-glutamine, 2 × 10^6 units mouse Leukemia inhibitory factor (mLif), 0.1 mM β-mercaptoethanol (Sigma), and antibiotics with or without 2i- PD0325901 (1 μM) and CHIR99021 (3 μM) (Tocris). For primary infection, MEFs were isolated from mice heterozygous for the reverse tetracycline-dependent transactivator (M2rtTA) that resides in the ubiquitously expressed *Gt(ROSA)26Sor* locus alone, or in combination with GFP that was either knocked-in to the *Sox2*, *Nanog*, or the *Oct4* locus. All infections were performed on MEFs (passage 0 or 1) that were seeded at 70% confluence 2 days prior to the first infection. Blastocyst-derived (bdTSC) lines were isolated as described (Oda et al., 2006). TSCs and stable iTSCs were grown in TSC culturing medium: a combined TSC medium containing 30% RPMI supplemented with 20% FBS, 1% non-essential amino acids, 2 mM L-glutamine, 25 ng/ml human recombinant FGF4 (PeproTech) and 1 μg/ml heparin (Sigma-Aldrich), and 70% MEF conditioned media (MEF-CM) with the same supplements. For culture of bdTSCs and stable iTSCs in defined medium, cells were grown on GFR-Matrigel-coated dishes in TX medium as described previously (Kubaczka et al., 2014). For differentiation experiments, DMEM supplemented with 10% FBS, 2 mM L-glutamine, and antibiotics was used. MEFs were directly converted into cardiomyocytes as previously reported (Efe et al., 2011). The joint ethics committee (IACUC) of the Hebrew University and Hadassah Medical Center approved the study protocol for animal welfare. The Hebrew University is an AAALAC international accredited institute.

Molecular Cloning, Lentiviral Infection, and Reprogramming to iTSCs

The 12 dox-inducible TSC factors were generated by cloning the open reading frame of each factor, obtained by reverse transcription with specific primers (see the Primer List in the Supplemental Information), into the TOPO-TA vector (Invitrogen) and then restricted with EcoRI or MfeI and inserted into the FUW-TetO expression vector.

For infection, replication-incompetent lentiviruses containing the GET factors (3.5 μg of each) or the GETM factors (3 μg of GET and 1 μg of M) were packaged with a lentiviral packaging mix (7.5 μg psPAX2 and 2.5 μg pGDM.2) in 293T cells and collected 48, 60, and 72 hr after transfection. The supernatants were filtered through a 0.45 μm filter, supplemented with 8 μg/ml of polybrene (Sigma), and then used to infect MEFs or TTFs. Six hours following the third infection, medium was replaced with fresh DMEM containing 10% FBS. Eighteen hours later, medium was replaced to TSC reprogramming medium (RPMI supplemented with 20% FBS, 0.1 mM β-mercaptoethanol, 2 mM L-glutamine, 25 ng/ml human recombinant FGF4 [PeproTech], 1 μg/ml heparin [Sigma-Aldrich], and 2 μg/ml doxycycline). TSC reprogramming medium was changed every other day for 20 days, followed by 10 days in TSC culturing medium (see above). Ten days after dox removal, plates were screened for primary iTSC colonies. Each colony was isolated, trypsinized, and plated in a separate well in a 6-well plate on feeder cells. Wells were followed and medium was replaced every other day for five to ten passages, until stable iTSC colonies developed.

Hemorrhagic Lesion Formation

A total of 5 × 10^6 iTSCs were resuspended in 100 μl CM containing hFGF4 and injected subcutaneously into male athymic nude mice. After 7 days, lesions were dissected, fixed in 4% paraformaldehyde overnight, embedded in paraffin, and sectioned (4 μm). Sections were stained with H&E and analyzed by a certified pathologist.

Chimeric Embryo and Placenta Contribution

Blastocyst injections were performed using CB6F1 host embryos. After priming with PMSG and hCG hormones and mating with CB6F1 males, embryos were obtained at 3.5 dpc (blastocyst stage) for chimera assay and 0.5 dpc (1-cell stage) and then cultured until 8-cell stage for staining. Embryos (0.5 dpc) were cultured in Evolve KSOMaa (Zenith Biotech) until reaching 8-cell stage embryo and then were injected with 10–20 bdTSCs or iTSCs. Eight-cell-stage embryos or 3.5 dpc blastocysts were injected with a flat tip microinjection pipette with an internal diameter of 16 μm (Origio) in drop of Evolve with HEPES KSOMaa (Zenith Biotech) medium under mineral oil. Shortly after injection, blastocysts were transferred to 2.5 dpc pseudopregnant CD1 females (~20 blastocysts per female). Eight-cell stage embryos were grown in Evolve KSOMaa (Zenith Biotech) until the blastocyst stage and then were fixed and subjected to immunostaining. Chimeric embryos or placentas were isolated at E13.5.

SUPPLEMENTAL INFORMATION

Supplemental Information includes Supplemental Experimental Procedures, six figures, one table, and two movies and can be found with this article online at http://dx.doi.org/10.1016/j.stem.2015.08.006.

AUTHOR CONTRIBUTIONS

Y.B. conceived the study. Y.B. and S.S. wrote the manuscript and prepared the figures. H.B., S.S., and Y.B. designed the experiments and performed cloning of the various factors, MEF infection, iTSC lines isolation from the various combinations of factors, FACS for cell-cycle analysis, hemorrhagic lesion assay, RNA preparation for RNA-seq, methylome analysis, and immunostaining for TSC markers. S.H. performed MEF infection and FACS for GFP sorting. N.v.W. and P.M.L. performed and analyzed the SCE and aneuploidy experiments. T.W. and A.X. performed and analyzed the H2A.X deposition experiments. N.M. and N.Y.T. performed the chromatin immunoprecipitation, direct conversion to cardiomyocytes, and immunostaining against Tnnt2. D.S. performed qPCR for TCS, ESC, epithelial, mesenchymal, and differentiation markers. D.S. and R.D. performed part of the methylome analysis. V.Z. performed part of the iTSC lines isolation. K.M. performed ESC and iTSC injections into blastocyst and determination of chimeric contributions.

ACKNOWLEDGMENTS

We thank Dr. Yuval Nevo and Dr. Sharona Elgavish of the Bioinformatics unit of the Hebrew University for computational and technical assistance. We also thank Dr. Shlomit Rak Yahalom from Rhenium for technical assistance with the Beckman Coulter flow cytometer. Y.B. is supported by a gift from the Morningstar Foundation and Edward & Millie Carew-Shaw Distinguished Medical Faculty Award and research grants from the Israeli Centers of Research Excellence (I-CORE) program (Center No. 41/11), the Israel Science Foundation (ISF), Kamin Fund, Abisch-Frenkel Foundation, and Alon Foundation Scholar-Program for distinguished junior faculty.

Received: January 6, 2015
Revised: June 25, 2015
Accepted: August 6, 2015
Published: September 24, 2015

REFERENCES

Adachi, K., Nikaido, I., Ohta, H., Ohtsuka, S., Ura, H., Kadota, M., Wakayama, T., Ueda, H.R., and Niwa, H. (2013). Context-dependent wiring of Sox2 regulatory networks for self-renewal of embryonic and trophoblast stem cells. Mol. Cell *52*, 380–392.

Anson-Cartwright, L., Dawson, K., Holmyard, D., Fisher, S.J., Lazzarini, R.A., and Cross, J.C. (2000). The glial cells missing-1 protein is essential for branching morphogenesis in the chorioallantoic placenta. Nat. Genet. *25*, 311–314.

Bar-Nur, O., Verheul, C., Sommer, A.G., Brumbaugh, J., Schwarz, B.A., Lipchina, I., Huebner, A.J., Mostoslavsky, G., and Hochedlinger, K. (2015). Lineage conversion induced by pluripotency factors involves transient passage through an iPSC stage. Nat. Biotechnol. *33*, 761–768.

Buganim, Y., Faddah, D.A., Cheng, A.W., Itskovich, E., Markoulaki, S., Ganz, K., Klemm, S.L., van Oudenaarden, A., and Jaenisch, R. (2012a). Single-cell expression analyses during cellular reprogramming reveal an early stochastic and a late hierarchic phase. Cell *150*, 1209–1222.

Buganim, Y., Itskovich, E., Hu, Y.C., Cheng, A.W., Ganz, K., Sarkar, S., Fu, D., Welstead, G.G., Page, D.C., and Jaenisch, R. (2012b). Direct reprogramming of fibroblasts into embryonic Sertoli-like cells by defined factors. Cell Stem Cell *11*, 373–386.

Buganim, Y., Faddah, D.A., and Jaenisch, R. (2013). Mechanisms and models of somatic cell reprogramming. Nat. Rev. Genet. *14*, 427–439.

Buganim, Y., Markoulaki, S., van Wietmarschen, N., Hoke, H., Wu, T., Ganz, K., Akhtar-Zaidi, B., He, Y., Abraham, B.J., Porubsky, D., et al. (2014). The developmental potential of iPSCs is greatly influenced by reprogramming factor selection. Cell Stem Cell *15*, 295–309.

Cahan, P., Li, H., Morris, S.A., Lummertz da Rocha, E., Daley, G.Q., and Collins, J.J. (2014). CellNet: network biology applied to stem cell engineering. Cell *158*, 903–915.

Cambuli, F., Murray, A., Dean, W., Dudzinska, D., Krueger, F., Andrews, S., Senner, C.E., Cook, S.J., and Hemberger, M. (2014). Epigenetic memory of the first cell fate decision prevents complete ES cell reprogramming into trophoblast. Nat. Commun. *5*, 5538.

Chen, L., Wang, D., Wu, Z., Ma, L., and Daley, G.Q. (2010). Molecular basis of the first cell fate determination in mouse embryogenesis. Cell Res. *20*, 982–993.

Cockburn, K., and Rossant, J. (2010). Making the blastocyst: lessons from the mouse. J. Clin. Invest. *120*, 995–1003.

Creyghton, M.P., Cheng, A.W., Welstead, G.G., Kooistra, T., Carey, B.W., Steine, E.J., Hanna, J., Lodato, M.A., Frampton, G.M., Sharp, P.A., et al. (2010). Histone H3K27ac separates active from poised enhancers and predicts developmental state. Proc. Natl. Acad. Sci. USA *107*, 21931–21936.

Efe, J.A., Hilcove, S., Kim, J., Zhou, H., Ouyang, K., Wang, G., Chen, J., and Ding, S. (2011). Conversion of mouse fibroblasts into cardiomyocytes using a direct reprogramming strategy. Nat. Cell Biol. *13*, 215–222.

Falconer, E., Hills, M., Naumann, U., Poon, S.S., Chavez, E.A., Sanders, A.D., Zhao, Y., Hirst, M., and Lansdorp, P.M. (2012). DNA template strand sequencing of single-cells maps genomic rearrangements at high resolution. Nat. Methods *9*, 1107–1112.

Genbacev, O., Lamb, J.D., Prakobphol, A., Donne, M., McMaster, M.T., and Fisher, S.J. (2013). Human trophoblast progenitors: where do they reside? Semin. Reprod. Med. *31*, 56–61.

James, J.L., Srinivasan, S., Alexander, M., and Chamley, L.W. (2014). Can we fix it? Evaluating the potential of placental stem cells for the treatment of pregnancy disorders. Placenta *35*, 77–84.

Kehler, J., Tolkunova, E., Koschorz, B., Pesce, M., Gentile, L., Boiani, M., Lomelí, H., Nagy, A., McLaughlin, K.J., Schöler, H.R., and Tomilin, A. (2004). Oct4 is required for primordial germ cell survival. EMBO Rep. *5*, 1078–1083.

Kibschull, M., Nassiry, M., Dunk, C., Gellhaus, A., Quinn, J.A., Rossant, J., Lye, S.J., and Winterhager, E. (2004). Connexin31-deficient trophoblast stem cells: a model to analyze the role of gap junction communication in mouse placental development. Dev. Biol. *273*, 63–75.

Kubaczka, C., Senner, C., Araúzo-Bravo, M.J., Sharma, N., Kuckenberg, P., Becker, A., Zimmer, A., Brüstle, O., Peitz, M., Hemberger, M., and Schorle, H. (2014). Derivation and maintenance of murine trophoblast stem cells under defined conditions. Stem Cell Reports *2*, 232–242.

Kuckenberg, P., Buhl, S., Woynecki, T., van Fürden, B., Tolkunova, E., Seiffe, F., Moser, M., Tomilin, A., Winterhager, E., and Schorle, H. (2010). The transcription factor TCFAP2C/AP-2gamma cooperates with CDX2 to maintain trophectoderm formation. Mol. Cell. Biol. *30*, 3310–3320.

Latos, P.A., and Hemberger, M. (2014). Review: the transcriptional and signalling networks of mouse trophoblast stem cells. Placenta *35* (*Suppl*), S81–S85.

Lee, T.I., and Young, R.A. (2013). Transcriptional regulation and its misregulation in disease. Cell *152*, 1237–1251.

Lin, C.Y., Lovén, J., Rahl, P.B., Paranal, R.M., Burge, C.B., Bradner, J.E., Lee, T.I., and Young, R.A. (2012). Transcriptional amplification in tumor cells with elevated c-Myc. Cell *151*, 56–67.

Lu, C.W., Yabuuchi, A., Chen, L., Viswanathan, S., Kim, K., and Daley, G.Q. (2008). Ras-MAPK signaling promotes trophectoderm formation from embryonic stem cells and mouse embryos. Nat. Genet. *40*, 921–926.

Montserrat, N., Nivet, E., Sancho-Martinez, I., Hishida, T., Kumar, S., Miquel, L., Cortina, C., Hishida, Y., Xia, Y., Esteban, C.R., and Izpisua Belmonte, J.C. (2013). Reprogramming of human fibroblasts to pluripotency with lineage specifiers. Cell Stem Cell *13*, 341–350.

Morris, S.A., Cahan, P., Li, H., Zhao, A.M., San Roman, A.K., Shivdasani, R.A., Collins, J.J., and Daley, G.Q. (2014). Dissecting engineered cell types and enhancing cell fate conversion via CellNet. Cell *158*, 889–902.

Ng, R.K., Dean, W., Dawson, C., Lucifero, D., Madeja, Z., Reik, W., and Hemberger, M. (2008). Epigenetic restriction of embryonic cell lineage fate by methylation of Elf5. Nat. Cell Biol. *10*, 1280–1290.

Nie, Z., Hu, G., Wei, G., Cui, K., Yamane, A., Resch, W., Wang, R., Green, D.R., Tessarollo, L., Casellas, R., et al. (2012). c-Myc is a universal amplifier of expressed genes in lymphocytes and embryonic stem cells. Cell *151*, 68–79.

Nishioka, N., Inoue, K., Adachi, K., Kiyonari, H., Ota, M., Ralston, A., Yabuta, N., Hirahara, S., Stephenson, R.O., Ogonuki, N., et al. (2009). The Hippo signaling pathway components Lats and Yap pattern Tead4 activity to distinguish mouse trophectoderm from inner cell mass. Dev. Cell *16*, 398–410.

Niwa, H., Miyazaki, J., and Smith, A.G. (2000). Quantitative expression of Oct-3/4 defines differentiation, dedifferentiation or self-renewal of ES cells. Nat. Genet. *24*, 372–376.

Niwa, H., Toyooka, Y., Shimosato, D., Strumpf, D., Takahashi, K., Yagi, R., and Rossant, J. (2005). Interaction between Oct3/4 and Cdx2 determines trophectoderm differentiation. Cell *123*, 917–929.

Oda, M., Shiota, K., and Tanaka, S. (2006). Trophoblast stem cells. Methods Enzymol. *419*, 387–400.

Ralston, A., Cox, B.J., Nishioka, N., Sasaki, H., Chea, E., Rugg-Gunn, P., Guo, G., Robson, P., Draper, J.S., and Rossant, J. (2010). Gata3 regulates trophoblast development downstream of Tead4 and in parallel to Cdx2. Development *137*, 395–403.

Russ, A.P., Wattler, S., Colledge, W.H., Aparicio, S.A., Carlton, M.B., Pearce, J.J., Barton, S.C., Surani, M.A., Ryan, K., Nehls, M.C., et al. (2000). Eomesodermin is required for mouse trophoblast development and mesoderm formation. Nature *404*, 95–99.

Shu, J., Wu, C., Wu, Y., Li, Z., Shao, S., Zhao, W., Tang, X., Yang, H., Shen, L., Zuo, X., et al. (2013). Induction of pluripotency in mouse somatic cells with lineage specifiers. Cell *153*, 963–975.

Simmons, D.G., and Cross, J.C. (2005). Determinants of trophoblast lineage and cell subtype specification in the mouse placenta. Dev. Biol. *284*, 12–24.

Simmons, D.G., Fortier, A.L., and Cross, J.C. (2007). Diverse subtypes and developmental origins of trophoblast giant cells in the mouse placenta. Dev. Biol. *304*, 567–578.

Soufi, A., Donahue, G., and Zaret, K.S. (2012). Facilitators and impediments of the pluripotency reprogramming factors' initial engagement with the genome. Cell *151*, 994–1004.

Sridharan, R., Tchieu, J., Mason, M.J., Yachechko, R., Kuoy, E., Horvath, S., Zhou, Q., and Plath, K. (2009). Role of the murine reprogramming factors in the induction of pluripotency. Cell *136*, 364–377.

Strumpf, D., Mao, C.A., Yamanaka, Y., Ralston, A., Chawengsaksophak, K., Beck, F., and Rossant, J. (2005). Cdx2 is required for correct cell fate specification and differentiation of trophectoderm in the mouse blastocyst. Development *132*, 2093–2102.

Takahashi, K., and Yamanaka, S. (2006). Induction of pluripotent stem cells from mouse embryonic and adult fibroblast cultures by defined factors. Cell *126*, 663–676.

Takashima, Y., Guo, G., Loos, R., Nichols, J., Ficz, G., Krueger, F., Oxley, D., Santos, F., Clarke, J., Mansfield, W., et al. (2014). Resetting transcription factor control circuitry toward ground-state pluripotency in human. Cell *158*, 1254–1269.

Tanaka, S., Kunath, T., Hadjantonakis, A.K., Nagy, A., and Rossant, J. (1998). Promotion of trophoblast stem cell proliferation by FGF4. Science *282*, 2072–2075.

Theunissen, T.W., Powell, B.E., Wang, H., Mitalipova, M., Faddah, D.A., Reddy, J., Fan, Z.P., Maetzel, D., Ganz, K., Shi, L., et al. (2014). Systematic identification of culture conditions for induction and maintenance of naive human pluripotency. Cell Stem Cell *15*, 471–487.

Wernig, M., Lengner, C.J., Hanna, J., Lodato, M.A., Steine, E., Foreman, R., Staerk, J., Markoulaki, S., and Jaenisch, R. (2008). A drug-inducible transgenic system for direct reprogramming of multiple somatic cell types. Nat. Biotechnol. *26*, 916–924.

Wu, T., Liu, Y., Wen, D., Tseng, Z., Tahmasian, M., Zhong, M., Rafii, S., Stadtfeld, M., Hochedlinger, K., and Xiao, A. (2014). Histone variant H2A.X deposition pattern serves as a functional epigenetic mark for distinguishing the developmental potentials of iPSCs. Cell Stem Cell *15*, 281–294.

Xu, J., Du, Y., and Deng, H. (2015). Direct lineage reprogramming: strategies, mechanisms, and applications. Cell Stem Cell *16*, 119–134.